Available online at www.sciencedirect.com

ScienceDirect

Procedia CIRP 75 (2018) 355–360

www.elsevier.com/locate/procedia

15th CIRP Conference on Computer Aided Tolerancing – CIRP CAT 2018

Uncertainty analysis of a six-degree-of-freedom surface encoder for a planar motion stage

Yuki Shimizu[a,]*, Masaya Furuta[a], Yuan-Liu Chen[a], Xiuguo Chen[a], Hiraku Matsukuma[a], Wei Gao[a]

[a]*Tohoku University, 6-6-01 Aramaki Aza-Aoba, Aoba-ku, Sendai, Miyagy, 980-8579 Japan*

* Corresponding author. Tel.: +81-22-795-6950; fax: +81-22-795-6953. *E-mail address:* yuki.shimizu@nano.mech.tohoku.ac.jp

Abstract

This paper presents an uncertainty analysis of a six-degree-of-freedom surface encoder, which is designed to measure multi-degree-of-freedom motion of a planar motion stage with a single laser beam. Since the surface encoder is composed of an optical sensor head and a two-axis scale grating, optical misalignments in the sensor head and form errors of the scale grating will affect the measurement uncertainty. In this paper, aiming to achieve further accurate measurement of translational displacement, an uncertainty budget table is built for the *X*-directional translational displacement measurement, while considering the above mentioned uncertainty sources.

Peer-review under responsibility of the Scientific Committee of the 15th CIRP Conference on Computer Aided Tolerancing - CIRP CAT 2018.

Keywords: Surface encoder; Uncertainty; Optical measurement

1. Introduction

Strong demands for miniaturization and multi-functionalization of electronic devices and optical devices can be found in modern industries. Semiconductor devices and optical elements are therefore desired to be miniaturized and/or to have complex freeform. In manufacturing equipments and measuring instruments for such products, ultra-precision positioning stages having nanometric positioning resolution, as well as multi-axis driving, a stroke longer than several hundreds of millimeter, and a nanometric positioning resolution, are necessary [1]. To satisfy these demands, a high-precision position measuring system, which can carry out simultaneous measurement of six-axis in real time, is required to be established so that a full-closed loop control of the stage system can be realized. Multi-axis measuring systems employing several single-axis sensors such as laser interferometers and capacitive sensors have therefore been constructed so far [2]. However, the integration of multiple sensors leads to an increase in the size and complexity of systems, and the installation error of each sensor degrades the measurement accuracy, as well. In addition, influences of the environment such as temperature deviation are crucial problems in the case of using laser interferometers.

In order to solve these problems, an optical sensor referred to as the six-degree-of-freedom (DOF) surface encoder has been developed [3]. With the enhancement of a two-dimensional (2D) scale grating and a reference grating, the surface encoder can carry out six-DOF measurement by using a single sensor head at a single measurement point. The optical system of the sensor consists of a displacement assembly for detection of three-axis translational displacements (*XYZ*) and an angle assembly for detection of three-axis angular displacements (θ_X, θ_Y, θ_Z). Experiments in the previous study have revealed that the developed six-axis surface encoder has a measurement resolution of 2 nm along the three axes (*XYZ*), 0.1 arc-second and 0.3 arc-second about the *XY*-axes (θ_X and θ_Y) and *Z*-axis (θ_Z), respectively [3].

Measurement of translational and angular displacements with the surface encoder will be affected by several uncertainty sources associated with optical misalignments in an optical sensor head of the surface encoder, form error of a two-dimensional diffraction grating employed as the scale

2212-8271 © 2018 The Authors. Published by Elsevier B.V.
Peer-review under responsibility of the Scientific Committee of the 15th CIRP Conference on Computer Aided Tolerancing - CIRP CAT 2018.
10.1016/j.procir.2018.04.041

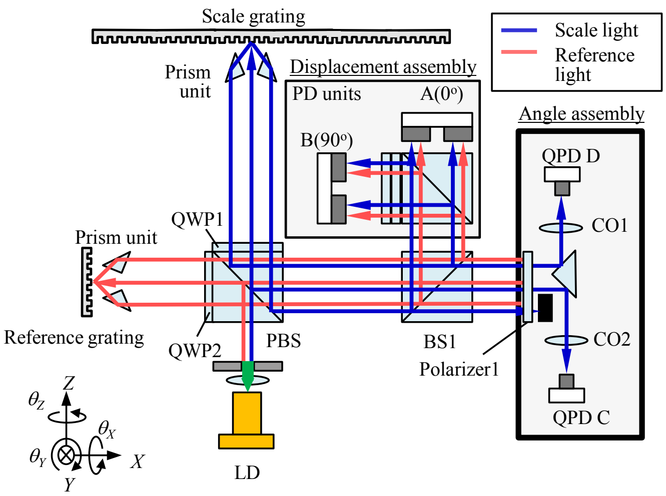

Fig. 1 A schematic of the optical configuration for the prototype optical sensor head of the six-DOF surface encoder [3]

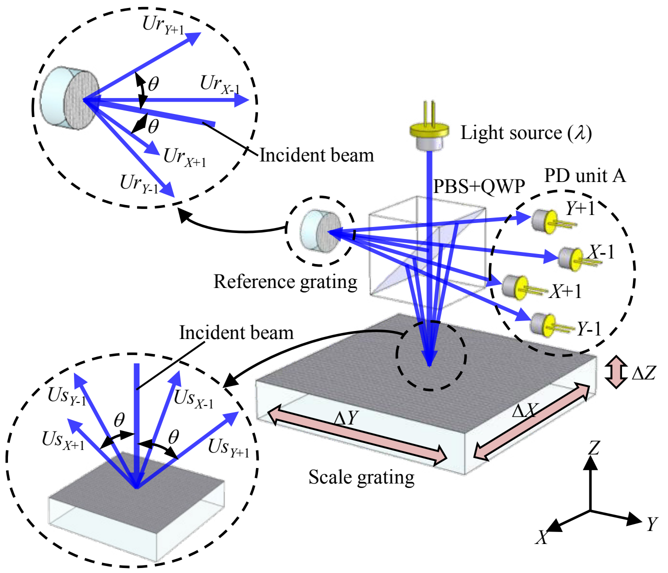

Fig. 2 A schematic of the displacement assembly and sources of uncertainty for measurement of three-DOF translational motion [3]

grating, environmental conditions and so on. In this paper, as the first step of uncertainty analysis of the six-DOF surface encoder, uncertainty of the *X*-directional translational displacement measurement is evaluated through some experiments with a developed prototype optical sensor head [3].

2. Principle of the surface encoder for measurement of six-degree-of-freedom position detection

A schematic of the optical design of six-DOF surface encoder is shown in Fig. 1 [3]. The surface encoder is composed of an angle assembly, a displacement assembly, a reference grating, a scale grating, and a laser diode (LD). In the setup, the reference grating is held stationary while the scale grating is mounted on a target of interest. The angle assembly measures three-DOF angular motion of the scale grating about the *X*-, *Y*- and *Z*-axes by utilizing a 0th- and 1st-order diffracted beams based on the principle of three-axis autocollimator [4]. Meanwhile, the displacement assembly measures translational motion of the scale grating along the *X*, *Y*, and *Z* directions. One of the main features of the six-DOF surface encoder is its optical configuration sharing a single laser beam from LD between the angle assembly and the displacement assembly. The optical design enables the surface encoder to carry out measurement complying with the Abbe principle [5], which is important for the next-generation precision positioning technology [6] that requires sub-nanometric positioning accuracy.

Figure 2 shows a schematic of the displacement assembly with the scale grating and the reference grating. In the displacement assembly, the first-order diffracted beams from the scale grating and those from the reference grating are made to superimpose with each other by using a polarized beam splitter (PBS) so that interference signals can be generated for measurement of translational motion of the scale grating. A laser beam emitted from the LD is divided into *p*- and *s*-polarized components by using the PBS. The *p*-polarized component goes through the PBS and is made incident to a scale grating, while the *s*-polarized component is reflected by the PBS and is made incident to a reference grating. The divided laser beams made incident to the 2D gratings generate first order diffracted beams in both the *X*- and *Y*-directions. Each of the diffracted beams from the scale grating is made to superimpose with each of ones from the reference grating by the PBS as shown in Fig. 2, and resulting four interference signals will be generated. By using the PD unit, each of the interference signals will be acquired independently.

Displacement of the scale grating along the *X*-, *Y*- and *Z*-directions will induce changes in the phases of diffracted beams from the scale grating. When the displacement ΔX along the *X*-direction is applied to the scale grating, the change in the phase of first order *X*-directional diffracted beams $\Omega_{X\pm1}$ will be as follows:

$$\Omega_{X\pm1} = \pm\frac{2\pi}{P}\Delta X \tag{1}$$

where *P* is the period of scale grating. In the same manner, the *Y*-directional displacement ΔY will generate a change in the phase of first order *Y*-directional diffracted beams $\Omega_{Y\pm1}$, which can be expressed as follows:

$$\Omega_{Y\pm1} = \pm\frac{2\pi}{P}\Delta Y \tag{2}$$

Meanwhile, in the case of the *Z*-directional displacement ΔZ, a phase change will be generated by the optical path difference (OPD) in between a path toward the scale grating and that toward the reference grating. Since the OPD generated by ΔZ will be $(1+\cos\theta)\Delta Z$, the change in phase Φ induced by ΔZ can be expressed as follows:

$$\Phi = (1+\cos\theta)\frac{2\pi}{\lambda}\Delta Z \tag{3}$$

where λ is the light wavelength, and θ is the first-order diffraction angle that can be calculated by the following equation:

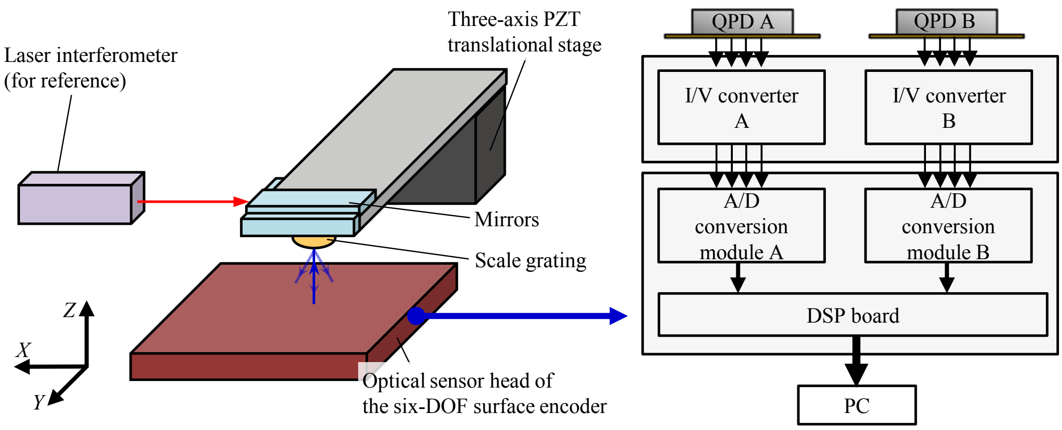

(a) A schematic of the experimental setup (b) Diagram of the signal processing

Fig. 3 A schematic and a photograph of the experimental setup

$$\theta = \sin^{-1}\left(\frac{\lambda}{P}\right) \tag{4}$$

It should be noted that ΔZ will induce the phase change Φ in each of the first order diffracted beams both in the X- and Y-directions. In summary, wavefronts of the X- and Y-directional first order diffracted beams $U_{s\alpha}$ (α=X+1, X-1, Y+1, Y-1) from the scale grating can be expressed as follows:

$$Us_{X\pm1} = U_0 \exp(i\Omega_{X\pm1}) \cdot \exp(i\Phi) \tag{5}$$

$$Us_{Y\pm1} = U_0 \exp(i\Omega_{Y\pm1}) \cdot \exp(i\Phi) \tag{6}$$

where U_0 is the amplitude of diffracted beam, which depends on the power of laser beam emitted from the LD. In addition, the wavefronts of the X- and Y-directional first order diffracted beams $U_{r\alpha}$ (α=X+1, X-1, Y+1, Y-1) from the reference grating can be expressed as follows:

$$Ur_{X+1} = Ur_{X-1} = Ur_{Y+1} = Ur_{Y-1} = U_0 \tag{7}$$

The wavefronts U_α resulting from superimpositions between the diffracted beams from the scale and reference gratings can therefore be expressed as follows:

$$U_{X\pm1} = Us_{X\pm1} + Ur_{X\pm1} \tag{8}$$

$$U_{Y\pm1} = Us_{Y\pm1} + Ur_{Y\pm1} \tag{9}$$

The interference signals I_α from the wavefronts U_α can be calculated as follows:

$$I_{X\pm1} = U_{X\pm1} \cdot \overline{U_{X\pm1}} = 2U_0^2\{1+\cos(\Omega_{X\pm1}+\Phi)\} \tag{10}$$

$$I_{Y\pm1} = U_{Y\pm1} \cdot \overline{U_{Y\pm1}} = 2U_0^2\{1+\cos(\Omega_{Y\pm1}+\Phi)\} \tag{11}$$

From these equations, the three-dimensional displacements ΔX, ΔY and ΔZ of the scale grating can be acquired. In the optical setup shown in Fig. 2, an additional PD unit (PD unit B), which detects interference signals having phase shifts of 90 degree with respect to those detected by the PD unit A, can be employed to distinguish the positive or negative direction of each of the translational motions [7]. It should be noted that the PD unit B is not indicated in the figure for the sake of simplicity. In summary, the three-dimensional displacements ΔX, ΔY and ΔZ of the scale grating can be detected from the interference signals detected by the PD units A ($S_{A\alpha\pm1}$) and B ($S_{B\alpha\pm1}$) as follows:

$$\Delta X = \frac{P}{4\pi}\left\{\arctan\left(\frac{S_{BX+1}}{S_{AX+1}}\right) - \arctan\left(\frac{S_{BX-1}}{S_{AX-1}}\right)\right\} \tag{12}$$

$$\Delta Y = \frac{P}{4\pi}\left\{\arctan\left(\frac{S_{BY+1}}{S_{AY+1}}\right) - \arctan\left(\frac{S_{BY-1}}{S_{AY-1}}\right)\right\} \tag{13}$$

$$\Delta Z = \frac{\lambda}{8\pi(1+\cos\theta)}\left\{\begin{array}{c}\arctan\left(\frac{S_{BX+1}}{S_{AX+1}}\right) + \arctan\left(\frac{S_{BX-1}}{S_{AX-1}}\right) + \\ \arctan\left(\frac{S_{BY+1}}{S_{AY+1}}\right) + \arctan\left(\frac{S_{BY-1}}{S_{AY-1}}\right)\end{array}\right\} \tag{14}$$

As can be seen in these equations, translational displacements along the X-, Y- and Z-directions can be obtained by detecting interference signals with the PD units.

3. Experiments for analysis of measurement uncertainty

3.1. Experimental setup

In this paper, the uncertainty in the measurement of translational displacement along the X-direction was evaluated based on GUM [8] throughout some experiments. Figures 3(a) shows a schematic of the experimental setup, and Fig. 3(b) shows a diagram of the signal processing employed in this paper to carry out analysis of measurement uncertainty of the multi-DOF surface encoder. As can be seen in the figure, an optical sensor head of the surface encoder was held stationary on a vibration-insulating table, while a scale grating having two-dimensional pattern structures was held by a supporting arm mounted on a three-axis piezoelectric (PZT) stage capable of giving translational motion to the scale

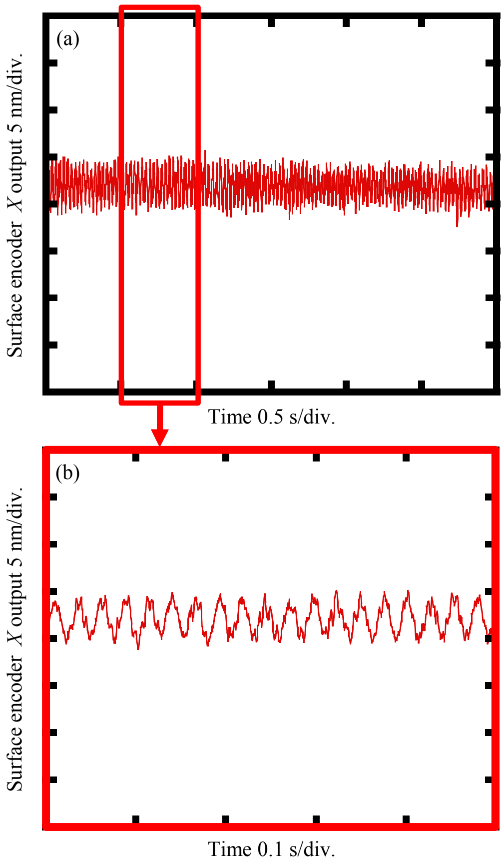

Fig. 4 Deviation of the surface encoder output

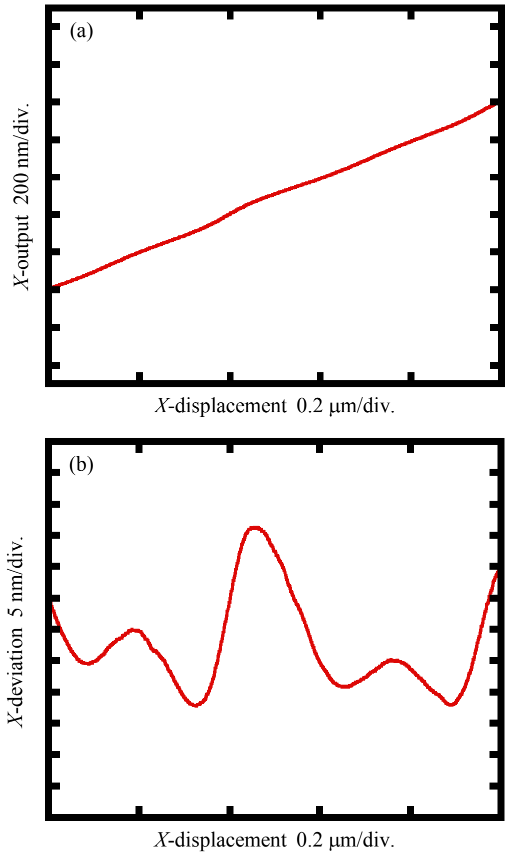

Fig. 5 Interpolation error

grating along the *X*-, *Y*- and *Z*-directions in the figure. In the setup, a commercial laser interferometer (Canon DS-80) was employed as a reference. A flat mirror was therefore attached to the supporting arm as the target mirror for the commercial laser interferometer. In this paper, uncertainty analysis is carried out focusing on the following four sources of uncertainty: (a) uncertainty due to short-term stability and electrical noise component, (b) uncertainty due to the interpolation error, (c) uncertainty due to the cross-talk, and (d) uncertainty due to the form errors of pattern structures of the 2D scale grating. Experimental data acquired by the setup are utilized to carry out uncertainty analysis for each of the sources of uncertainty.

3.2. Uncertainty due to each of the sources of uncertainty

(a) Short-term stability and electrical noise components in the surface encoder outputs

Voltage outputs from the optical sensor head of the multi-DOF surface encoder are affected by external disturbances such as mechanical vibrations, the change in ambient temperature, and so on. In addition, electromagnetic disturbances induced by several factors such as instability of the laser diode employed as the light source for the optical sensor head or a noise component in the output from the DC stabilized power supply could also affect the surface encoder output. Although it is not so easy to evaluate a degree of the influence of each of the uncertainty sources, a sum of these influences can be experimentally evaluated by evaluating the stabilities of the surface encoder outputs. Figure 4(a) shows output deviations of the surface encoder captured during 3 seconds with a sampling rate of 2 kHz. Figure 4(b) shows the close up of the plot in Fig. 4(a). As can be seen in the figure, a component with a frequency of 50 Hz was found to be the main cause of the output deviation. The standard deviation was evaluated to be 1.333 nm. Since the value of a single observation will be employed as the surface encoder output, the standard uncertainty associated with the stability and noise components in the surface encoder outputs $u(e_{\mathrm{Stability}})$ is evaluated to be $u(e_{\mathrm{Stability}}) / \sqrt{1}$ =1.333 nm.

(b) Interpolation error

Interpolation error of the surface encoder was determined experimentally by using the setup shown in Fig. 3. Linear motion with a constant velocity of 250 nm/s along the *X*-direction was given to the scale grating mounted on the PZT stage, while monitoring the *X*-displacement of the scale grating by the surface encoder, with the commercial laser interferometer employed as a reference. Sampling rates of both the surface encoder output and the reference laser interferometer output were set to be 1 kHz. Figure 5(a) shows the result. In the figure, the horizontal axis is the *X*-displacement of the scale grating measured by the reference laser interferometer, while the vertical axis is the *X*-displacement of the scale grating measured by the surface encoder. It should be noted that the sensor output is influenced by a misalignment between the surface encoder and the laser interferometer. The linear component is eliminated and the plot in Fig. 5(a) was re-plotted as shown in Fig. 5(b). It should be noted that a high-frequency component

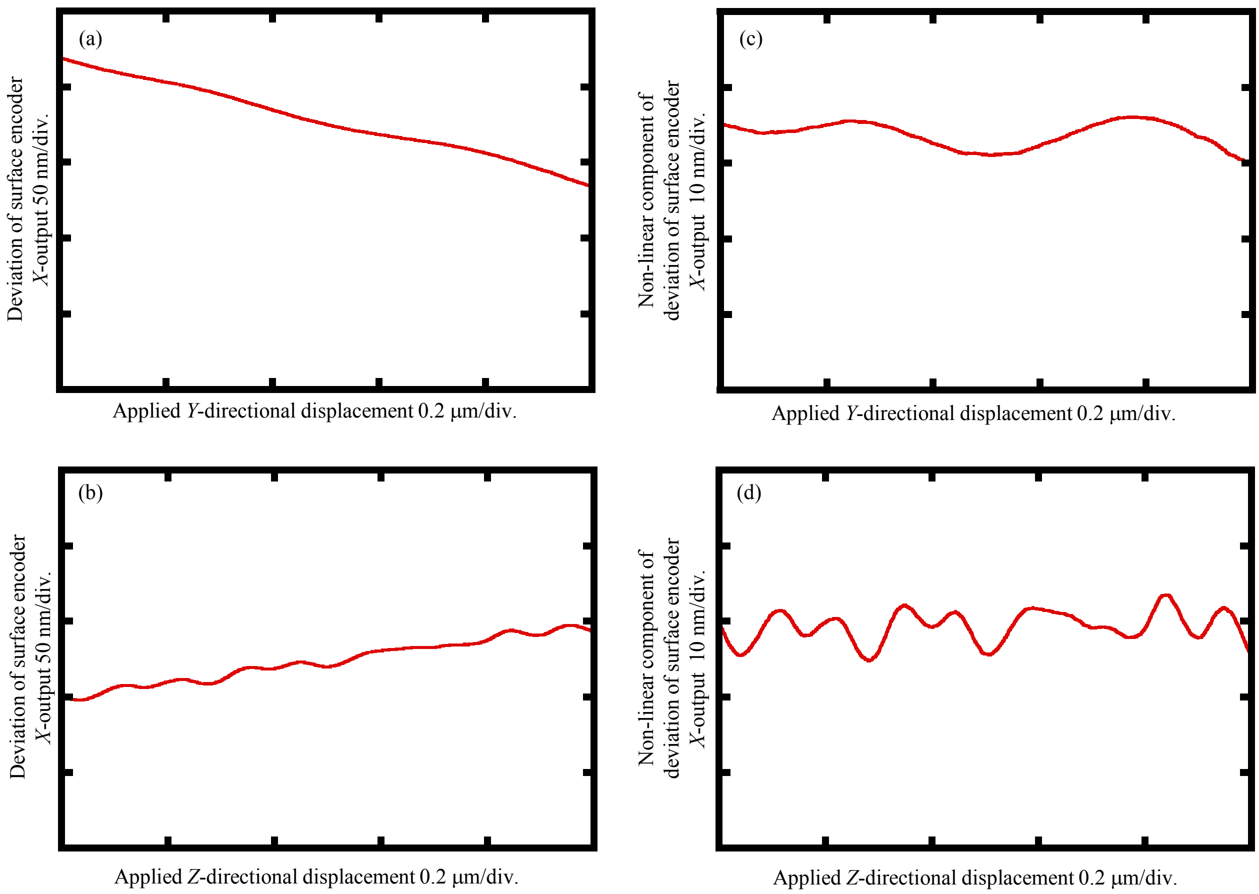

Fig. 6 Evaluation of the crosstalk error

in the surface encoder output is eliminated by calculating 100-point simple moving average. Interpolation errors were evaluated to be ±14.2 nm. Regarding the graduation periods of the surface encoder outputs (570 nm for the *X*- and *Y*-directions), the interpolation errors were evaluated to be ±2.50% for measurement of the *X*-directional displacement. The standard uncertainty associated with the interpolation error $u(e_{\mathrm{Interpolation}})$ is evaluated by using the experimental results described above. By regarding the probability distribution as rectangular, $u(e_{\mathrm{Interpolation}})=14.2/\sqrt{3}=8.198$ nm.

(c) Crosstalk among the *X*-, *Y*- and *Z*-axes

Crosstalks among the *X*-, *Y*- and *Z*-axes in the surface encoder were evaluated in experiments by using the setup shown in Fig. 3. Experiments including the signal processing for the surface encoder output were carried out in the same manner as the evaluation of interpolation error. Translational motion with a constant velocity of 250 nm/s was given to the scale grating along a specific direction (the *Y*- or *Z*-direction), while detecting the motion of the scale grating along the *X*-direction by the surface encoder. Figures 6(a) and 6(b) show the deviations of the surface encoder output when translational motion along each of the *Y*- and *Z*-directions was applied to the scale grating. As can be seen in the figures, each deviation of surface encoder output had a linear component, which is mainly due to a misalignment between the local coordinate systems of the PZT actuator and the surface encoder. Orthogonal error of the two-dimensional pattern structures in the scale grating could also affect the deviations. Meanwhile, influences of these linear components in the surface encoder can be compensated by carrying out calibration in advance of the measurement. Therefore, in this paper, a non-linear component of the deviations of surface encoder *X*-output is evaluated by eliminating the linear component as shown in Fig. 6(c) and 6(d). As can be seen in the figures, the maximum crosstalk error was found to be 8.77 nm. The standard uncertainty associated with the crosstalk $u(e_{\mathrm{Crosstalk}})$ is evaluated by using the experimental results. By regarding the probability distribution as rectangular, $u(e_{\mathrm{Crosstalk}})=8.77/2\sqrt{3}=3.101$ nm.

(d) Form errors of pattern structures of the 2D scale grating

In the surface encoder, the *X*-directional periods of pattern structures on the scale grating are employed as scale graduations of the translational displacements along the *X*-direction. Deviations of grating periods could therefore be sources of uncertainty. By using a fast evaluation method based on a Fizeau interferometer [9], the *X*-directional grating period deviation of the scale grating employed in this paper was evaluated over an area of 25 mm×25 mm. The deviation of grating periods along the *X*-direction was evaluated to be 70 nm. According to the results, the measurement error due to the form error of the scale grating is expected to be approximately 0.00028% at the most. Therefore, regarding the probability distribution as rectangular, the standard uncertainty associated with the form error of the scale grating

Table 1 Uncertainty for translational motion measurement

Source of uncertainty	Symbol	Type	Probability distribution	Divisor	Standard uncertainty	Sensitivity coefficient	$\lvert c(x_i)\rvert \times u(x_i)$ nm
Stability and noise component	$u(e_{\text{Stability}})$	A	—	—	1.333 nm	1	1.333
Interpolation error	$u(e_{\text{Interpolation}})$	B	Rectangular	$\sqrt{3}$	8.198 nm	1	8.198
Crosstalk	$u(e_{\text{Crosstalk}})$	B	Rectangular	$2\sqrt{3}$	3.101 nm	1	3.101
Grating form	$u(e_{\text{Grating}})$	B	Rectangular	$2\sqrt{3}$	0.808 nm	1	0.808
Combined standard uncertainty	U_c			—			8.902
Expanded uncertainty ($k = 2$)	U			—			17.804

$u(e_{\text{Grating}})$ can be calculated as $u(e_{\text{Grating}})=L\times 2.8\times 10^{-6}/2\sqrt{3}$, where L is the measurement range. If we assume that L=1000 μm, $u(e_{\text{Grating}})$=0.808 nm.

Regarding the above calculated standard uncertainties, the combined uncertainty U_c is calculated as follows:

$$U_c = \sqrt{u^2(e_{\text{Stability}}) + u^2(e_{\text{Interpolation}}) + u^2(e_{\text{Crosstalk}}) + u^2(e_{\text{Grating}})} = \sqrt{1.333^2 + 8.198^2 + 3.101^2 + 0.808^2} = 8.902 \text{ nm} \tag{15}$$

For a coverage factor of k=2, multiply the combined standard uncertainty by 2, to give an expanded uncertainty U of 17.804 nm (95% confidence). Uncertainties due to those sources of uncertainty analyzed as described above are summarized as shown in Table 1. It should be noted that the uncertainty analysis was carried out focusing on the X-directional translational displacement measurement. In addition, influences of the other factors such as long-term stability of the sensor output which could be affected by environmental conditions have not been taken into consideration in this paper. Further detailed analysis will be carried out as future work, as well as the establishment of a mathematical model considering transfer functions of the multi-DOF surface encoder system.

4. Conclusions

In this paper, an uncertainty analysis of a six-degree-of-freedom surface encoder for a planar motion stage has been carried out based on GUM by using results acquired in the evaluation experiments of a prototype multi-DOF surface encoder. The analysis has been carried out focusing on the influences of short-term stability and electrical noises, interpolation error, cross-talk, and form errors of pattern structures of the 2D scale grating.

Acknowledgements

This research is supported by Japan Society for the Promotion of Science (JSPS).

References

[1] Gao W, Kim SW, Bosse H, Haitjema H, Chen YL, Lu XD, Knapp W, Weckenmann A, Estler WT and Kunzmann H. Measurement technologies for precision engineering. CIRP Ann Manuf Technol 2015;64(2):773-796.
[2] T. Oiwa, M. Katsuki, M. Karita, W. Gao, S. Makinouchi, K. Sato, Y. Oohashi. Report of Questionnaire Survey on Ultra-precision Positioning. Technical Committee of Ultra-Precision Positioning. Japan Society for Precision Engineering (JSPE); 2015.
[3] Li X, Gao W, Muto H, Shimizu Y, Ito S, Dian S. A six-degree-of-freedom surface encoder for precision positioning of a planar motion stage. Precis Eng 2013;37:771-81.
[4] Gao W, Saito Y, Muto H, Arai Y and Shimizu Y. A three-axis autocollimator for detection of angular error motions of a precision stage. CIRP Ann Manuf Technol 2011;60-1:515-8.
[5] Bryan JB. The Abbe Principle Revisited: An Updated Interpretation. Precis Eng 1979;1(3):129-132.
[6] Jäger G, Manske E, Hausotte T, Müller A and Balzer F. Surf Topogr Metrol Prop 2016;4:034004.
[7] Gao W. Precision Nanometrology - Sensors and Measuring Systems for Nanomanufacturing. London: Springer; pp. 109-128, 2010.
[8] JCGM 100:2008 Evaluation of Measurement Data - Guide to the Expression of Uncertainty in Measurement (GUM); 2008.
[9] Gao W, Kimura A. A fast evaluation method for pitch deviation and out-of-flatness of a planar scale grating. CIRP Ann Manuf Technol 2000;59(1):505-508.